

Measurement of $\cos 2\beta$ in $B^0 \rightarrow D^{(*)0}h^0$ decays with a time-dependent
Dalitz plot analysis of $D^0 \rightarrow K_s^0\pi^+\pi^-$

The *BABAR* Collaboration

November 21, 2006

Abstract

We report a preliminary measurement of $\cos 2\beta$ in $B^0 \rightarrow D^{(*)0}h^0$ decays with a time-dependent Dalitz plot analysis of $D^0 \rightarrow K_s^0\pi^+\pi^-$, where h^0 is a light neutral meson such as π^0 , η , η' or ω . The strong phase variation on the Dalitz plot allows the access to the angle β with only a two-fold ambiguity ($\beta + \pi$). Using 311×10^6 $B\bar{B}$ pairs collected at the *BABAR* detector, we obtain $\cos 2\beta = 0.54 \pm 0.54 \pm 0.08 \pm 0.18$, $\sin 2\beta = 0.45 \pm 0.36 \pm 0.05 \pm 0.07$, and $|\lambda| = 0.975_{-0.085}^{+0.093} \pm 0.012 \pm 0.002$, where the first errors are statistical, the second are experimental systematic uncertainties, and the third are the signal Dalitz model uncertainties. This measurement favors the solution of $\beta = 22^\circ$ over 68° at an 87% confidence level.

Submitted to the 33rd International Conference on High-Energy Physics, ICHEP 06,
26 July—2 August 2006, Moscow, Russia.

Stanford Linear Accelerator Center, Stanford University, Stanford, CA 94309

Work supported in part by Department of Energy contract DE-AC03-76SF00515.

The BABAR Collaboration,

B. Aubert, R. Barate, M. Bona, D. Boutigny, F. Couderc, Y. Karyotakis, J. P. Lees, V. Poireau,
V. Tisserand, A. Zghiche

*Laboratoire de Physique des Particules, IN2P3/CNRS et Université de Savoie, F-74941 Annecy-Le-Vieux,
France*

E. Grauges

Universitat de Barcelona, Facultat de Física, Departament ECM, E-08028 Barcelona, Spain

A. Palano

Università di Bari, Dipartimento di Fisica and INFN, I-70126 Bari, Italy

J. C. Chen, N. D. Qi, G. Rong, P. Wang, Y. S. Zhu

Institute of High Energy Physics, Beijing 100039, China

G. Eigen, I. Ofte, B. Stugu

University of Bergen, Institute of Physics, N-5007 Bergen, Norway

G. S. Abrams, M. Battaglia, D. N. Brown, J. Button-Shafer, R. N. Cahn, E. Charles, M. S. Gill,
Y. Groysman, R. G. Jacobsen, J. A. Kadyk, L. T. Kerth, Yu. G. Kolomensky, G. Kukartsev, G. Lynch,
L. M. Mir, T. J. Orimoto, M. Pripstein, N. A. Roe, M. T. Ronan, W. A. Wenzel

Lawrence Berkeley National Laboratory and University of California, Berkeley, California 94720, USA

P. del Amo Sanchez, M. Barrett, K. E. Ford, A. J. Hart, T. J. Harrison, C. M. Hawkes, S. E. Morgan,
A. T. Watson

University of Birmingham, Birmingham, B15 2TT, United Kingdom

T. Held, H. Koch, B. Lewandowski, M. Pelizaeus, K. Peters, T. Schroeder, M. Steinke
Ruhr Universität Bochum, Institut für Experimentalphysik 1, D-44780 Bochum, Germany

J. T. Boyd, J. P. Burke, W. N. Cottingham, D. Walker

University of Bristol, Bristol BS8 1TL, United Kingdom

D. J. Asgeirsson, T. Cuhadar-Donszelmann, B. G. Fulsom, C. Hearty, N. S. Knecht, T. S. Mattison,
J. A. McKenna

University of British Columbia, Vancouver, British Columbia, Canada V6T 1Z1

A. Khan, P. Kyberd, M. Saleem, D. J. Sherwood, L. Teodorescu

Brunel University, Uxbridge, Middlesex UB8 3PH, United Kingdom

V. E. Blinov, A. D. Bukin, V. P. Druzhinin, V. B. Golubev, A. P. Onuchin, S. I. Serednyakov,
Yu. I. Skovpen, E. P. Solodov, K. Yu Todyshev

Budker Institute of Nuclear Physics, Novosibirsk 630090, Russia

D. S. Best, M. Bondioli, M. Bruinsma, M. Chao, S. Curry, I. Eschrich, D. Kirkby, A. J. Lankford, P. Lund,
M. Mandelkern, R. K. Mommsen, W. Roethel, D. P. Stoker

University of California at Irvine, Irvine, California 92697, USA

S. Abachi, C. Buchanan

University of California at Los Angeles, Los Angeles, California 90024, USA

S. D. Foulkes, J. W. Gary, O. Long, B. C. Shen, K. Wang, L. Zhang
University of California at Riverside, Riverside, California 92521, USA

H. K. Hadavand, E. J. Hill, H. P. Paar, S. Rahatlou, V. Sharma
University of California at San Diego, La Jolla, California 92093, USA

J. W. Berryhill, C. Campagnari, A. Cunha, B. Dahmes, T. M. Hong, D. Kovalskyi, J. D. Richman
University of California at Santa Barbara, Santa Barbara, California 93106, USA

T. W. Beck, A. M. Eisner, C. J. Flacco, C. A. Heusch, J. Kroseberg, W. S. Lockman, G. Nesom, T. Schalk,
B. A. Schumm, A. Seiden, P. Spradlin, D. C. Williams, M. G. Wilson
University of California at Santa Cruz, Institute for Particle Physics, Santa Cruz, California 95064, USA

J. Albert, E. Chen, A. Dvoretzkii, F. Fang, D. G. Hitlin, I. Narsky, T. Piatenko, F. C. Porter, A. Ryd,
A. Samuel
California Institute of Technology, Pasadena, California 91125, USA

G. Mancinelli, B. T. Meadows, K. Mishra, M. D. Sokoloff
University of Cincinnati, Cincinnati, Ohio 45221, USA

F. Blanc, P. C. Bloom, S. Chen, W. T. Ford, J. F. Hirschauer, A. Kreisel, M. Nagel, U. Nauenberg,
A. Olivas, W. O. Ruddick, J. G. Smith, K. A. Ulmer, S. R. Wagner, J. Zhang
University of Colorado, Boulder, Colorado 80309, USA

A. Chen, E. A. Eckhart, A. Soffer, W. H. Toki, R. J. Wilson, F. Winklmeier, Q. Zeng
Colorado State University, Fort Collins, Colorado 80523, USA

D. D. Altenburg, E. Feltresi, A. Hauke, H. Jasper, J. Merkel, A. Petzold, B. Spaan
Universität Dortmund, Institut für Physik, D-44221 Dortmund, Germany

T. Brandt, V. Klose, H. M. Lacker, W. F. Mader, R. Nogowski, J. Schubert, K. R. Schubert, R. Schwierz,
J. E. Sundermann, A. Volk
Technische Universität Dresden, Institut für Kern- und Teilchenphysik, D-01062 Dresden, Germany

D. Bernard, G. R. Bonneaud, E. Latour, Ch. Thiebaux, M. Verderi
Laboratoire Leprince-Ringuet, CNRS/IN2P3, Ecole Polytechnique, F-91128 Palaiseau, France

P. J. Clark, W. Gradl, F. Muheim, S. Playfer, A. I. Robertson, Y. Xie
University of Edinburgh, Edinburgh EH9 3JZ, United Kingdom

M. Andreotti, D. Bettoni, C. Bozzi, R. Calabrese, G. Cibinetto, E. Luppi, M. Negrini, A. Petrella,
L. Piemontese, E. Prencipe
Università di Ferrara, Dipartimento di Fisica and INFN, I-44100 Ferrara, Italy

F. Anulli, R. Baldini-Ferroli, A. Calcaterra, R. de Sangro, G. Finocchiaro, S. Pacetti, P. Patteri,
I. M. Peruzzi,¹ M. Piccolo, M. Rama, A. Zallo
Laboratori Nazionali di Frascati dell'INFN, I-00044 Frascati, Italy

¹Also with Università di Perugia, Dipartimento di Fisica, Perugia, Italy

A. Buzzo, R. Capra, R. Contri, M. Lo Vetere, M. M. Macri, M. R. Monge, S. Passaggio, C. Patrignani,
E. Robutti, A. Santroni, S. Tosi

Università di Genova, Dipartimento di Fisica and INFN, I-16146 Genova, Italy

G. Brandenburg, K. S. Chaisanguanthum, M. Morii, J. Wu

Harvard University, Cambridge, Massachusetts 02138, USA

R. S. Dubitzky, J. Marks, S. Schenk, U. Uwer

Universität Heidelberg, Physikalisches Institut, Philosophenweg 12, D-69120 Heidelberg, Germany

D. J. Bard, W. Bhimji, D. A. Bowerman, P. D. Dauncey, U. Egede, R. L. Flack, J. A. Nash,
M. B. Nikolich, W. Panduro Vazquez

Imperial College London, London, SW7 2AZ, United Kingdom

P. K. Behera, X. Chai, M. J. Charles, U. Mallik, N. T. Meyer, V. Ziegler

University of Iowa, Iowa City, Iowa 52242, USA

J. Cochran, H. B. Crawley, L. Dong, V. Eyges, W. T. Meyer, S. Prell, E. I. Rosenberg, A. E. Rubin

Iowa State University, Ames, Iowa 50011-3160, USA

A. V. Gritsan

Johns Hopkins University, Baltimore, Maryland 21218, USA

A. G. Denig, M. Fritsch, G. Schott

Universität Karlsruhe, Institut für Experimentelle Kernphysik, D-76021 Karlsruhe, Germany

N. Arnaud, M. Davier, G. Grosdidier, A. Höcker, F. Le Diberder, V. Lepeltier, A. M. Lutz, A. Oyanguren,
S. Pruvot, S. Rodier, P. Roudeau, M. H. Schune, A. Stocchi, W. F. Wang, G. Wormser

*Laboratoire de l'Accélérateur Linéaire, IN2P3/CNRS et Université Paris-Sud 11, Centre Scientifique
d'Orsay, B.P. 34, F-91898 ORSAY Cedex, France*

C. H. Cheng, D. J. Lange, D. M. Wright

Lawrence Livermore National Laboratory, Livermore, California 94550, USA

C. A. Chavez, I. J. Forster, J. R. Fry, E. Gabathuler, R. Gamet, K. A. George, D. E. Hutchcroft,
D. J. Payne, K. C. Schofield, C. Touramanis

University of Liverpool, Liverpool L69 7ZE, United Kingdom

A. J. Bevan, F. Di Lodovico, W. Menges, R. Sacco

Queen Mary, University of London, E1 4NS, United Kingdom

G. Cowan, H. U. Flaecher, D. A. Hopkins, P. S. Jackson, T. R. McMahon, S. Ricciardi, F. Salvatore,
A. C. Wren

*University of London, Royal Holloway and Bedford New College, Egham, Surrey TW20 0EX, United
Kingdom*

D. N. Brown, C. L. Davis

University of Louisville, Louisville, Kentucky 40292, USA

J. Allison, N. R. Barlow, R. J. Barlow, Y. M. Chia, C. L. Edgar, G. D. Lafferty, M. T. Naisbit,
J. C. Williams, J. I. Yi

University of Manchester, Manchester M13 9PL, United Kingdom

C. Chen, W. D. Hulsbergen, A. Jawahery, C. K. Lae, D. A. Roberts, G. Simi

University of Maryland, College Park, Maryland 20742, USA

G. Blaylock, C. Dallapiccola, S. S. Hertzbach, X. Li, T. B. Moore, S. Saremi, H. Staengle

University of Massachusetts, Amherst, Massachusetts 01003, USA

R. Cowan, G. Sciolla, S. J. Sekula, M. Spitznagel, F. Taylor, R. K. Yamamoto

*Massachusetts Institute of Technology, Laboratory for Nuclear Science, Cambridge, Massachusetts 02139,
USA*

H. Kim, S. E. McLachlin, P. M. Patel, S. H. Robertson

McGill University, Montréal, Québec, Canada H3A 2T8

A. Lazzaro, V. Lombardo, F. Palombo

Università di Milano, Dipartimento di Fisica and INFN, I-20133 Milano, Italy

J. M. Bauer, L. Cremaldi, V. Eschenburg, R. Godang, R. Kroeger, D. A. Sanders, D. J. Summers,
H. W. Zhao

University of Mississippi, University, Mississippi 38677, USA

S. Brunet, D. Côté, M. Simard, P. Taras, F. B. Viaud

Université de Montréal, Physique des Particules, Montréal, Québec, Canada H3C 3J7

H. Nicholson

Mount Holyoke College, South Hadley, Massachusetts 01075, USA

N. Cavallo,² G. De Nardo, F. Fabozzi,³ C. Gatto, L. Lista, D. Monorchio, P. Paolucci, D. Piccolo,
C. Sciacca

Università di Napoli Federico II, Dipartimento di Scienze Fisiche and INFN, I-80126, Napoli, Italy

M. A. Baak, G. Raven, H. L. Snoek

*NIKHEF, National Institute for Nuclear Physics and High Energy Physics, NL-1009 DB Amsterdam, The
Netherlands*

C. P. Jessop, J. M. LoSecco

University of Notre Dame, Notre Dame, Indiana 46556, USA

T. Allmendinger, G. Benelli, L. A. Corwin, K. K. Gan, K. Honscheid, D. Hufnagel, P. D. Jackson,
H. Kagan, R. Kass, A. M. Rahimi, J. J. Regensburger, R. Ter-Antonyan, Q. K. Wong

Ohio State University, Columbus, Ohio 43210, USA

N. L. Blount, J. Brau, R. Frey, O. Igonkina, J. A. Kolb, M. Lu, R. Rahmat, N. B. Sinev, D. Strom,
J. Strube, E. Torrence

University of Oregon, Eugene, Oregon 97403, USA

²Also with Università della Basilicata, Potenza, Italy

³Also with Università della Basilicata, Potenza, Italy

A. Gaz, M. Margoni, M. Morandin, A. Pompili, M. Posocco, M. Rotondo, F. Simonetto, R. Stroili, C. Voci
Università di Padova, Dipartimento di Fisica and INFN, I-35131 Padova, Italy

M. Benayoun, H. Briand, J. Chauveau, P. David, L. Del Buono, Ch. de la Vaissière, O. Hamon,
B. L. Hartfiel, M. J. J. John, Ph. Leruste, J. Malcès, J. Ocariz, L. Roos, G. Therin
*Laboratoire de Physique Nucléaire et de Hautes Energies, IN2P3/CNRS, Université Pierre et Marie
Curie-Paris6, Université Denis Diderot-Paris7, F-75252 Paris, France*

L. Gladney, J. Panetta
University of Pennsylvania, Philadelphia, Pennsylvania 19104, USA

M. Biasini, R. Covarelli
Università di Perugia, Dipartimento di Fisica and INFN, I-06100 Perugia, Italy

C. Angelini, G. Batignani, S. Bettarini, F. Bucci, G. Calderini, M. Carpinelli, R. Cenci, F. Forti,
M. A. Giorgi, A. Lusiani, G. Marchiori, M. A. Mazur, M. Morganti, N. Neri, G. Rizzo, J. J. Walsh
Università di Pisa, Dipartimento di Fisica, Scuola Normale Superiore and INFN, I-56127 Pisa, Italy

M. Haire, D. Judd, D. E. Wagoner
Prairie View A&M University, Prairie View, Texas 77446, USA

J. Biesiada, N. Danielson, P. Elmer, Y. P. Lau, C. Lu, J. Olsen, A. J. S. Smith, A. V. Telnov
Princeton University, Princeton, New Jersey 08544, USA

F. Bellini, G. Cavoto, A. D'Orazio, D. del Re, E. Di Marco, R. Faccini, F. Ferrarotto, F. Ferroni,
M. Gaspero, L. Li Gioi, M. A. Mazzoni, S. Morganti, G. Piredda, F. Polci, F. Safai Tehrani, C. Voena
Università di Roma La Sapienza, Dipartimento di Fisica and INFN, I-00185 Roma, Italy

M. Ebert, H. Schröder, R. Waldi
Universität Rostock, D-18051 Rostock, Germany

T. Adye, N. De Groot, B. Franek, E. O. Olaiya, F. F. Wilson
Rutherford Appleton Laboratory, Chilton, Didcot, Oxon, OX11 0QX, United Kingdom

R. Aleksan, S. Emery, A. Gaidot, S. F. Ganzhur, G. Hamel de Monchenault, W. Kozanecki, M. Legendre,
G. Vasseur, Ch. Yèche, M. Zito
DSM/Daphnia, CEA/Saclay, F-91191 Gif-sur-Yvette, France

X. R. Chen, H. Liu, W. Park, M. V. Purohit, J. R. Wilson
University of South Carolina, Columbia, South Carolina 29208, USA

M. T. Allen, D. Aston, R. Bartoldus, P. Bechtle, N. Berger, R. Claus, J. P. Coleman, M. R. Convery,
M. Cristinziani, J. C. Dingfelder, J. Dorfan, G. P. Dubois-Felsmann, D. Dujmic, W. Dunwoodie,
R. C. Field, T. Glanzman, S. J. Gowdy, M. T. Graham, P. Grenier,⁴ V. Halyo, C. Hast, T. Hryn'ova,
W. R. Innes, M. H. Kelsey, P. Kim, D. W. G. S. Leith, S. Li, S. Luitz, V. Luth, H. L. Lynch,
D. B. MacFarlane, H. Marsiske, R. Messner, D. R. Muller, C. P. O'Grady, V. E. Ozcan, A. Perazzo,
M. Perl, T. Pulliam, B. N. Ratcliff, A. Roodman, A. A. Salnikov, R. H. Schindler, J. Schwiening,
A. Snyder, J. Stelzer, D. Su, M. K. Sullivan, K. Suzuki, S. K. Swain, J. M. Thompson, J. Va'vra, N. van

⁴Also at Laboratoire de Physique Corpusculaire, Clermont-Ferrand, France

Bakel, M. Weaver, A. J. R. Weinstein, W. J. Wisniewski, M. Wittgen, D. H. Wright, A. K. Yarritu, K. Yi,
C. C. Young

Stanford Linear Accelerator Center, Stanford, California 94309, USA

P. R. Burchat, A. J. Edwards, S. A. Majewski, B. A. Petersen, C. Roat, L. Wilden

Stanford University, Stanford, California 94305-4060, USA

S. Ahmed, M. S. Alam, R. Bula, J. A. Ernst, V. Jain, B. Pan, M. A. Saeed, F. R. Wappler, S. B. Zain

State University of New York, Albany, New York 12222, USA

W. Bugg, M. Krishnamurthy, S. M. Spanier

University of Tennessee, Knoxville, Tennessee 37996, USA

R. Eckmann, J. L. Ritchie, A. Satpathy, C. J. Schilling, R. F. Schwitters

University of Texas at Austin, Austin, Texas 78712, USA

J. M. Izen, X. C. Lou, S. Ye

University of Texas at Dallas, Richardson, Texas 75083, USA

F. Bianchi, F. Gallo, D. Gamba

Università di Torino, Dipartimento di Fisica Sperimentale and INFN, I-10125 Torino, Italy

M. Bomben, L. Bosisio, C. Cartaro, F. Cossutti, G. Della Ricca, S. Dittongo, L. Lanceri, L. Vitale

Università di Trieste, Dipartimento di Fisica and INFN, I-34127 Trieste, Italy

V. Azzolini, N. Lopez-March, F. Martinez-Vidal

IFIC, Universitat de Valencia-CSIC, E-46071 Valencia, Spain

Sw. Banerjee, B. Bhuyan, C. M. Brown, D. Fortin, K. Hamano, R. Kowalewski, I. M. Nugent, J. M. Roney,
R. J. Sobie

University of Victoria, Victoria, British Columbia, Canada V8W 3P6

J. J. Back, P. F. Harrison, T. E. Latham, G. B. Mohanty, M. Pappagallo

Department of Physics, University of Warwick, Coventry CV4 7AL, United Kingdom

H. R. Band, X. Chen, B. Cheng, S. Dasu, M. Datta, K. T. Flood, J. J. Hollar, P. E. Kutter, B. Mellado,
A. Mihalyi, Y. Pan, M. Pierini, R. Prepost, S. L. Wu, Z. Yu

University of Wisconsin, Madison, Wisconsin 53706, USA

H. Neal

Yale University, New Haven, Connecticut 06511, USA

1 INTRODUCTION

The Standard Model of electroweak interactions describes charge-parity (CP) violation as a consequence of an irreducible phase in the three-generation Cabibbo-Kobayashi-Maskawa (CKM) quark-mixing matrix [1]. In this framework, the CP parameter $\sin 2\beta$ can be measured by examining the proper-time distribution of neutral B decays to CP eigenstates. This parameter has been measured with a high precision by the B -factories using final states containing a charmonium and a neutral kaon [2]. The current average from B -factories is $\sin 2\beta = 0.685 \pm 0.032$ [3], which leads to a four-fold solution of the angle $\beta = 22^\circ, 68^\circ, (22^\circ + 180^\circ),$ and $(68^\circ + 180^\circ)$. The ambiguity can leave possible new physics undetected even with very high precision measurements of $\sin 2\beta$.

Analyses have been attempted to resolve the $(\beta, \pi/2 - \beta)$ ambiguity using a time-dependent angular analysis in $B^0 \rightarrow J/\psi K^{*0}(K_S^0\pi^0)$ decays [4]. In this analysis we use a new method proposed by Bondar *et al.* [5], which uses $B^0 \rightarrow D^{(*)0}h^0$ decays with a time-dependent Dalitz plot analysis of $D^0 \rightarrow K_S^0\pi^+\pi^-$, where h^0 is a light neutral meson such as $\pi^0, \eta^{(\prime)},$ and ω . This method takes advantage of the varying strong phase on the $D^0 \rightarrow K_S^0\pi^+\pi^-$ Dalitz plot to resolve the ambiguity of the phase 2β from the $\sin 2\beta$ measurements alone. The Belle Collaboration has recently reported a measurement using this technique [6]; they obtained $\cos 2\beta = 1.87_{-0.53}^{+0.40+0.22}$ and determined the sign of $\cos 2\beta$ to be positive at a 98.3% confidence level.

The leading order diagram of $B^0 \rightarrow D^{(*)0}h^0$ is color-suppressed, as shown in Figure 1. The next order diagram is suppressed by $\mathcal{O}(\sin^2 \theta_{\text{Cabibbo}})$. There are no penguin diagram contributions. A sizable new physics effect due to supersymmetry without R-parity is possible in $b \rightarrow \bar{u}d$ decays, while the Standard Model uncertainty is relatively small [7]. Interference between $B^0 \rightarrow \bar{D}^0h^0$ and $B^0 \rightarrow \bar{B}^0 \rightarrow D^0h^0$ via mixing occurs when D^0 and \bar{D}^0 decay to a common final state, such as $K_S^0\pi^+\pi^-$.

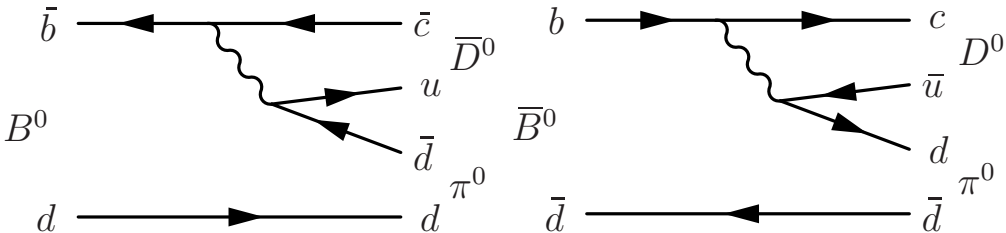


Figure 1: Leading diagrams for $B^0 \rightarrow D^0 h^0$ decays.

Assuming CPT symmetry is conserved and the decay rate difference $\Delta\Gamma$ is negligible, the time evolution function for a state that is known to be a B^0 at a time $t = t_{\text{tag}}$ can be expressed as

$$|B_{\text{phys}}^0(t)\rangle = e^{-\Gamma\Delta t/2} \left[|B^0\rangle \cos(\Delta m\Delta t/2) + i\frac{q}{p} |\bar{B}^0\rangle \sin(\Delta m\Delta t/2) \right], \quad (1)$$

where Γ is the average decay rate of the two mass eigenstates of B^0 meson, Δm is the mixing frequency, $\Delta t = t_{\text{rec}} - t_{\text{tag}}$ is the time difference between B^0 decay time t_{rec} and t_{tag} , and q/p is the ratio of $|\bar{B}^0\rangle$ and $|B^0\rangle$ coefficients in B^0 mass eigenstates. Neglecting CP violation in B^0 mixing, we assume $|q/p| = 1$. Expressing the decay amplitude of the decay chain $B^0 \rightarrow \bar{D}^0 h^0 \rightarrow [K_S^0\pi^+\pi^-]h^0$ as $A_f = AA_{\bar{D}}$ and similarly for \bar{B}^0 as $\bar{A}_{\bar{f}} = \bar{A}A_D$, the decay probability of a neutral B meson in

an $\Upsilon(4S)$ system can be shown to be

$$\mathcal{P}_{\pm} = \frac{1}{2}e^{-\Gamma\Delta t}|A|^2 \cdot \left[(|A_{\overline{D}}|^2 + |\lambda|^2|A_D|^2) \mp (|A_{\overline{D}}|^2 - |\lambda|^2|A_D|^2) \cos(\Delta m\Delta t) \right. \\ \left. \pm 2|\lambda|\eta_{h^0}(-1)^L \text{Im}\left(e^{-2i\beta} A_D A_{\overline{D}}^*\right) \sin(\Delta m\Delta t) \right], \quad (2)$$

where the upper (lower) sign is for B^0 (\overline{B}^0)-tagged events, $\lambda = \frac{q\overline{A}_T}{pA_f}$, $-2i\beta$ is the phase of q/p , η_{h^0} is the CP eigenvalue of h^0 , and L is the orbital angular momentum in the $D^{(*)0}h^0$ system. In the case of $B^0 \rightarrow D^{*0}h^0$ (where h^0 is a pseudoscalar) with $D^{*0} \rightarrow D^0\pi^0$, $L = 1$ and two additional factors need to be considered: the angular momentum in $D^{*0} \rightarrow D^0\pi^0$ ($L' = 1$) and the CP eigenvalue of the soft π^0 from D^{*0} decay ($\eta_{\pi^0} = -1$) [9]. The decay amplitudes A_D and $A_{\overline{D}}$ can be expressed as a function of two Lorentz invariant variables $m_+^2 \equiv (p_{K_S^0} + p_{\pi^+})^2$ and $m_-^2 \equiv (p_{K_S^0} + p_{\pi^-})^2$. That is, $A_D = A_D(m_+^2, m_-^2)$ and $A_{\overline{D}} = A_D(m_-^2, m_+^2)$. Here we have assumed that CP is conserved in the D^0 decay and neglected D^0 mixing.

In the last term of Equation(2), one can rewrite

$$\text{Im}\left(e^{-2i\beta} A_D A_{\overline{D}}^*\right) = \text{Im}(A_D A_{\overline{D}}^*) \cos 2\beta - \text{Re}(A_D A_{\overline{D}}^*) \sin 2\beta, \quad (3)$$

and treat $\cos 2\beta$ and $\sin 2\beta$ as independent parameters.

In this analysis, we use an unbinned maximum-likelihood method to fit for $\cos 2\beta$, $\sin 2\beta$ and $|\lambda|$, and use a parameterized Monte Carlo method based on the observed data to estimate the confidence level of $\cos 2\beta$ being positive.

2 THE BABAR DETECTOR AND DATASET

This analysis is based on 311×10^6 $B\overline{B}$ pairs collected on the $\Upsilon(4S)$ resonance during 1999–2006 with the BABAR detector at the PEP-II storage ring. A sample of 23 fb^{-1} collected at 40 MeV below the $\Upsilon(4S)$ resonance and a number of signal and generic simulation samples based on Geant4 [10] are also analyzed to optimize the event selection and to study background properties.

The BABAR detector is described in detail elsewhere [11]. Charged-particle trajectories are measured by a five-layer double-sided silicon vertex tracker and a 40-layer drift chamber located within a 1.5 T solenoidal magnetic field. Charged hadrons are identified by combining energy-loss information from the tracking system with the measurements from a ring-imaging Cherenkov detector. Photons are detected by a CsI(Tl) crystal electromagnetic calorimeter with an energy resolution of $\sigma_E/E = 0.023(E/\text{GeV})^{-1/4} \oplus 0.014$. The magnetic flux return is instrumented for muon and K_L^0 identification.

3 EVENT RECONSTRUCTION AND SELECTION

In this analysis, we reconstruct B^0 decays to D^0h^0 , where $h^0 = \pi^0(\gamma\gamma)$, $\eta(\gamma\gamma, \pi^+\pi^-\pi^0)$, $\eta'(\pi^+\pi^-\eta)$, and $\omega(\pi^+\pi^-\pi^0)$, and $B^0 \rightarrow D^{*0}(\rightarrow D^0\pi^0)h^0$, where $h^0 = \pi^0(\gamma\gamma)$ and $\eta(\gamma\gamma)$. The D^0 is reconstructed in $K_S^0\pi^+\pi^-$ mode.

A charged track must be reconstructed in the drift chamber, and, if it does not result from a K_S^0 decay, it must extrapolate back to within 1.5 cm of the nominal interaction point in the plane transverse to the beam and 10 cm along the beam. A cluster found in the calorimeter that is not

associated with a charged track is considered a photon candidate if its shower shape is consistent with a photon and its energy is greater than 30 MeV.

The π^0 candidates are reconstructed by combining two photon candidates with the $\gamma\gamma$ invariant mass in the range 110–160 MeV/ c^2 if used in $D^{*0} \rightarrow D^0\pi^0$ reconstruction, or 115–150 MeV/ c^2 if used in $B^0 \rightarrow D^{(*)0}\pi^0$ reconstruction; for the latter, each of the two photons is required to have an energy greater than 50 MeV. For $\eta \rightarrow \gamma\gamma$, the photon candidates must both have an energy greater than 100 MeV and the photon pair must have an invariant mass within 40 MeV/ c^2 of the nominal η mass [12] and have a momentum greater than 200 MeV/ c in the laboratory frame. If the $\eta \rightarrow \gamma\gamma$ candidate is later used in a $D^{*0}\eta$ candidate, the mass window is tightened to 33 MeV/ c^2 . The η candidate is removed if the invariant mass of one of the photons and another photon in the rest of the event is within 6 MeV/ c^2 of the nominal π^0 mass. For $\eta \rightarrow \pi^+\pi^-\pi^0$, the invariant mass of the candidate is required to be within 9 MeV/ c of the nominal η mass. An η' candidate is formed by combining an η candidate with two pions. The invariant mass must be within 8 MeV/ c^2 of the nominal η' mass. An ω candidate is formed by combining $\pi^+\pi^-\pi^0$. The invariant mass of the three-pion candidate is required to be within 18 MeV/ c^2 of the nominal ω mass. The π^0 candidate used in ω reconstruction is required to have a momentum greater than 200 MeV/ c in the laboratory frame. Except for ω , all h^0 are fitted with their mass constrained at the nominal value.

A K_S^0 candidate consists of a vertexed pair of oppositely-charged tracks with an invariant mass within 12 MeV/ c^2 of the nominal K_S^0 mass with a χ^2 probability greater than 0.1%. The K_S^0 flight distance must be greater than three times the estimated uncertainty, and the angle between the flight direction and the vertex displacement from the beam spot in the transverse plane must satisfy $\cos\theta > 0.992$.

A D^0 candidate consists of a pair of oppositely-charged tracks and a K_S^0 candidate. The invariant mass, m_{D^0} , must be within 60 MeV/ c^2 of the nominal D^0 mass. The m_{D^0} resolution is approximately 7 MeV/ c^2 . We retain the sideband for later use in the fit. We then fit the D^0 kinematic parameters with both D^0 and K_S^0 constrained at their respective nominal mass. These D^0 candidates are combined with a π^0 to form a D^{*0} candidate. The invariant mass is required to be within 3.0 (2.8) MeV/ c^2 of the D^{*0} nominal mass in $B^0 \rightarrow D^{*0}\pi^0$ ($D^{*0}\eta$) reconstruction.

Eventually we build a B^0 candidate combining a π^0 , η , ω or η' with a D^0 or a D^{*0} candidate. We fit the B^0 decay vertex requiring that the production vertex is consistent with the beam spot in the transverse plane. The energy-substituted mass $m_{\text{ES}} \equiv \sqrt{(s/2 + \mathbf{p}_0 \cdot \mathbf{p}_B)^2/E_0^2 - |\mathbf{p}_B|^2}$ is required to be greater than 5.2 GeV/ c^2 , where s is the squared center-of-mass (c.m.) energy, (E_0 , \mathbf{p}_0) and (E_B , \mathbf{p}_B) are the four-momentum of the initial state e^+e^- and the B candidate, respectively. The energy difference $\Delta E \equiv E_B - E_{\text{beam}}^*$, evaluated in the c.m. frame, must be between ± 80 MeV (± 40 MeV) for events with $h^0 \rightarrow \gamma\gamma$ ($h^0 \rightarrow \pi^+\pi^-\pi^0$ and $\eta' \rightarrow \pi^+\pi^-\eta$).

The majority of the background is from $q\bar{q}$ continuum events. We suppress them by requiring the normalized second order Fox-Wolfram moment R_2 [13] to be less than 0.5 and $|\cos\theta_T|$ less than 0.9, where θ_T is the angle between the thrust of the B candidate and the thrust of the rest of the event. We further suppress the continuum events by a Fisher discriminant formed from the following five variables: $\cos\theta_T$, the B flight angle in the c.m. frame, total event sphericity, total event thrust magnitude, and the ratio of two moments L_2/L_0 , where $L_i = \sum_j p_j^* |\cos\theta_j^*|^i$, summed over the remaining particles j in the event, where θ_j^* and p_j^* are the angle with respect to the B^0 thrust and the momentum in the c.m. frame. For $D^0\omega$ events, two variables are added to take advantage of the polarization of the ω : the angle between the B flight direction and the normal to the three-pion plane in the $\omega \rightarrow \pi^+\pi^-\pi^0$ rest frame, and the angle between one pion in the rest frame of the remaining pion pair with respect to the direction of the pion pair. The

Fisher coefficients are calculated using off-resonance data and simulated signal event samples. The optimum selection value is determined mode by mode by maximizing the signal yield significance using simulated signal and generic background events.

For $B^0 \rightarrow D^{(*)0}\pi^0$, one major background source is the color-allowed decay $B^+ \rightarrow D^0\rho^+$, which has a branching fraction approximately 50 times larger. For events reconstructed as a $D^0\pi^0$, the $D^0\rho^+$ contribution peaks in ΔE below the selection region and only a small number of events is selected. However, for events reconstructed as a $D^{*0}\pi^0$, the final state $D^0\pi^0\pi^0$ is very similar to $D^0(\pi^0\pi^+)_{\rho^+}$. Therefore this background has a mean ΔE near zero. We veto $B^+ \rightarrow D^0\rho^+$ events by rejecting $D^{*0}\pi^0$ candidates if the π^0 candidate combined with any other charged pion in the event can form a ρ^+ candidate with an invariant mass within 250 MeV/ c^2 of the nominal value, and subsequently form a B^+ candidate by combining with the D^0 candidate. The requirements for the B^+ candidate are $m_{\text{ES}} > 5.27$ GeV/ c^2 and $|\Delta E| < 100$ MeV. Finally, we only retain events with decay time difference $|\Delta t| < 15$ ps and the estimated uncertainty $\sigma_{\Delta t} < 3.6$ ps. If there is more than one candidate in the event, the one with a more signal-like Fisher discriminant is selected.

We use a two-dimensional (m_{ES}, m_{D^0}) probability density function (PDF) in an unbinned-maximum-likelihood fit to separate three types of events: (1) signal: a single Gaussian in m_{ES} and a Crystal Ball function [15] in m_{D^0} ; (2) combinatorial background with a real D^0 : an Argus [14] function in m_{ES} and a Crystal Ball function in m_{D^0} ; (3) combinatorial background with a combinatorial D^0 : an Argus function in m_{ES} and a first order polynomial in m_{D^0} . The Crystal Ball parameters for m_{D^0} in components (1) and (2) share the same values, as does the Argus parameter in (2) and (3).

The results of the fit are shown in Figures 2 and 3; the yields are shown in Table 1. We merge the $D^0\eta$ and $D^0\eta'$ samples, as well as the $D^{*0}\pi^0$ and $D^{*0}\eta$ samples. The Dalitz distributions in the signal region and m_{ES} sideband are shown in Figure 4. There are irreducible backgrounds that peak in both m_{ES} and m_{D^0} , which cannot be discriminated against with our PDF. The majority of this peaking background is from $B^+ \rightarrow D^{(*)0}\rho^+$. We estimate the amount of the peaking background using the simulated generic Monte Carlo samples. The number of signal events after subtracting the peaking background is shown in the last row in Table 1.

Table 1: Signal event yields.

Decay mode	$D^0\pi^0$	$D^0\eta, \eta'$	$D^0\omega$	$D^{*0}\pi^0, \eta$	Total
Raw peak yield	175 ± 17	97 ± 11	93 ± 12	59 ± 9	424 ± 25
Peaking background subtracted yield	168 ± 19	87 ± 12	82 ± 13	47 ± 9	384 ± 28

4 DALITZ PLOT MODEL

The D^0 decay amplitude is determined from an unbinned maximum-likelihood fit to a high-purity sample of $D^{*+} \rightarrow D^0\pi^+$ decays. We use the isobar formalism described in [16] to express A_D as a sum of two-body decay matrix element (subscript r) and a non-resonant (subscript NR) contribution,

$$A_D(m_+^2, m_-^2) = \sum_r a_r e^{i\phi_r} A_r(m_+^2, m_-^2) + a_{\text{NR}} e^{i\phi_{\text{NR}}}, \quad (4)$$

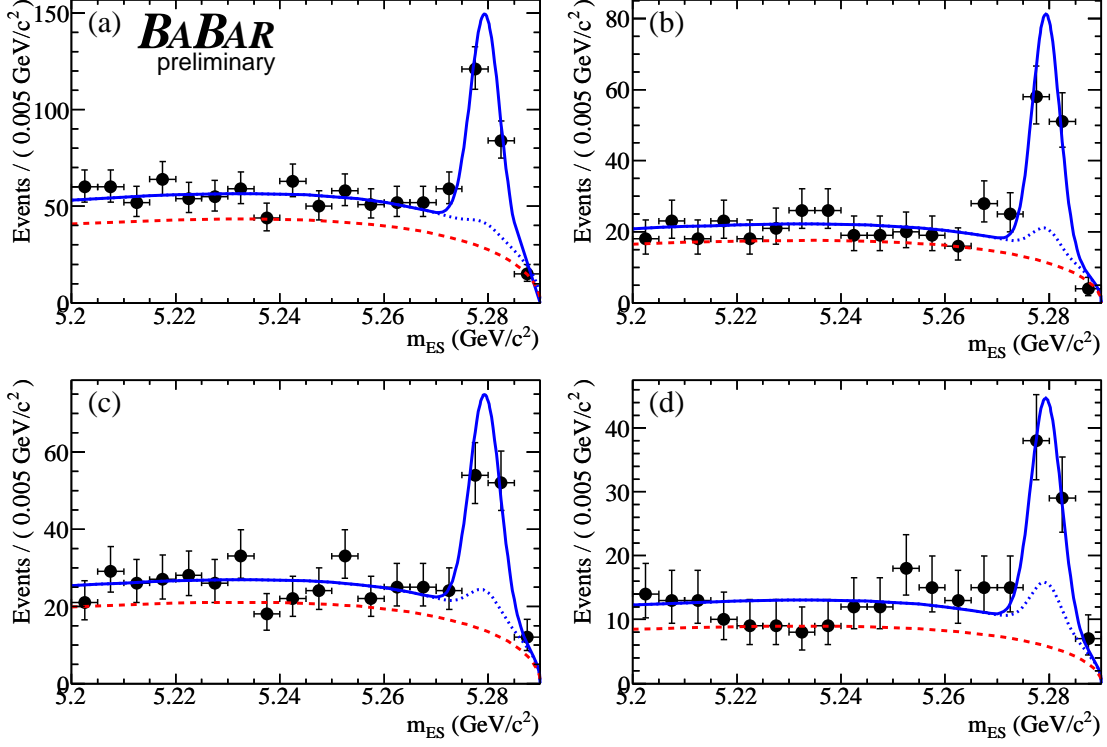


Figure 2: Distributions of m_{ES} for (a) $D^0\pi^0$, (b) $D^0\eta^{(\prime)}$, (c) $D^0\omega$ and (d) $D^{*0}\pi^0, \eta$ for events with m_{D^0} within 14 MeV/c^2 of the nominal value. Curves are: (solid) overall PDF projection; (dotted) background (including peaking) PDF; (dashed) contribution from background with fake D^0 .

where each term is parameterized with an amplitude a_r and a phase ϕ_r . The function $A_r(m_+^2, m_-^2)$ is the Lorentz-invariant expression for the matrix element of a D^0 meson decaying into $K_S^0\pi^+\pi^-$ through an intermediate resonance r , parameterized as a function of the position in the Dalitz plane.

The resonances in the model for D^0 are: (a) [$K_S^0\pi^-$] resonances: $K^*(892)^-$, $K_0^*(1430)^-$, $K_2^*(1430)^-$, $K^*(1410)^-$, and $K^*(1680)^-$; (b) [$K_S^0\pi^+$] resonances (doubly-Cabibbo suppressed): $K^*(892)^+$, $K_0^*(1430)^+$, and $K_2^*(1430)^+$; (c) [$\pi^+\pi^-$] resonances: $\rho(770)$, $\omega(782)$, $f_0(980)$, $f_0(1370)$, $f_2(1270)$, $\rho(1450)$ and two scalar resonances σ and σ' . For $\rho(770)$ and $\rho(1450)$ we use the functional form suggested in [18], while the remaining resonances are parameterized by a spin-dependent relativistic Breit-Wigner distribution. The means and widths of the resonances are taken from the PDG [12], except for σ and σ' , which are obtained from the Dalitz plot fit. The inclusion of σ and σ' significantly improves the Dalitz plot fit quality. However, since these two scalars are not well established, we consider the systematic effect of using a model without them. More details about the Dalitz plot model and parameters can be found in [17]. We neglect the detector resolution in the Dalitz plot model because the resolution ($\simeq 4 \text{ (MeV}/c^2)^2$) is much smaller than the resonance widths. Only $\omega(782)$ has an intrinsic width comparable to the mass resolution. We increase its width artificially in the systematic study.

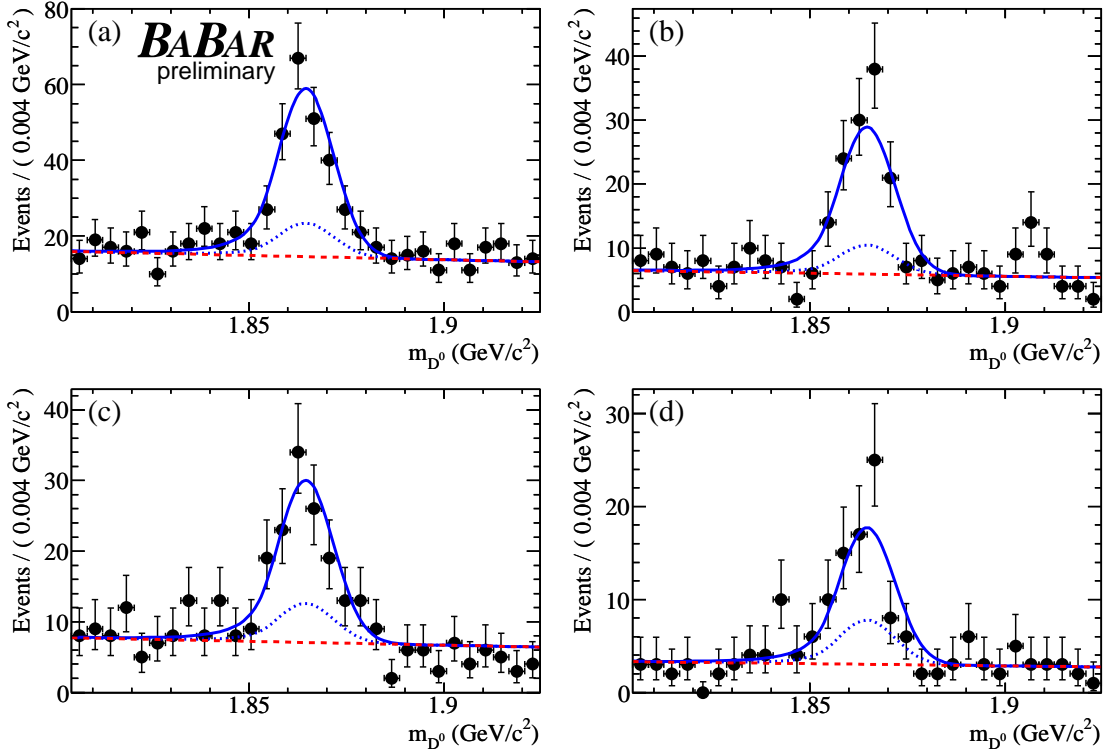


Figure 3: Distributions of m_{D^0} for (a) $D^0\pi^0$, (b) $D^0\eta^{(\prime)}$, (c) $D^0\omega$ and (d) $D^{*0}\pi^0, \eta$ for events with $m_{ES} > 5.27$ GeV/c^2 . Curves are: (solid) overall PDF projection; (dotted) background (including peaking) PDF; (dashed) contribution from background with fake D^0 .

5 TIME-DEPENDENT ANALYSIS

We model the time-dependent Dalitz plot distribution in a PDF that consists of four components: signal, background with a real D^0 , background with a fake D^0 and background that peaks in both m_{ES} and m_{D^0} . The (m_{ES}, m_{D^0}) model for the first three components has been described in Section 3. The peaking background component shares the same (m_{ES}, m_{D^0}) shape with the signal component. The background fractions are determined from a fit to (m_{ES}, m_{D^0}) distributions and from generic Monte Carlo samples (for peaking background) for each B^0 mode group and each tagging category. Each event is assigned signal and background probabilities based on the two-dimensional PDF.

The time-dependent Dalitz model for signal is based on Equation(2). We modify the equation to take into account mistagging and imperfect Δt reconstruction, following the methods used in our other time-dependent analyses [19], i.e., an additional factor $(1 - 2w)$ is added to the $\cos(\Delta m \Delta t)$ and $\sin(\Delta m \Delta t)$ terms, and the equation is convolved with a three-Gaussian Δt resolution function. There are six tagging categories with different mistag fractions w . We also allow the w of each category to be different for B^0 and \bar{B}^0 tags. The means and widths of the core and the second Gaussian are parameterized with scale factors multiplied by $\sigma_{\Delta t}$. The mean and width of the third (outlier) Gaussian are fixed at 0 ps and 8 ps, respectively. The mistag rates and the resolution function are determined from control samples of $B^0 \rightarrow D^{(*)}\pi, \rho, a_1$ decays. Most of the resolution

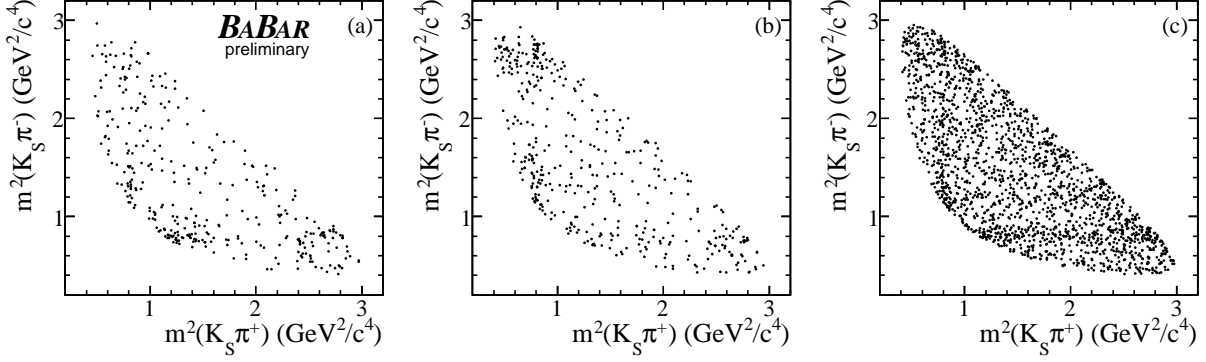


Figure 4: Dalitz distributions for (a) B^0 -tagged and (b) \bar{B}^0 -tagged events in the signal region, $m_{\text{ES}} > 5.27 \text{ GeV}/c^2$, and (c) events in the m_{ES} sideband $m_{\text{ES}} < 5.26 \text{ GeV}/c^2$. In all cases, the D^0 mass is required to be within $20 \text{ MeV}/c^2$ of the nominal value.

function parameters are consistent among the six tagging categories, except for the core Gaussian mean and scale factor, where the Lepton tagged sample is significantly different from others. We allow these two parameters to be different for Lepton tag.

The model for the background with a fake D^0 is determined from the D^0 sideband data. The Δt model consists of a prompt component and an exponential decay component with an effective lifetime. The resolution function is a Gaussian whose mean and width are scaled by $\sigma_{\Delta t}$, plus an outlier Gaussian. The mean of the core Gaussian and the fraction of the prompt component are allowed to be different between the Lepton tag and the other tags.

The Dalitz distribution for background is modeled by an incoherent mixture of several resonances and a phase-space distribution,

$$\mathcal{P}(m_+^2, m_-^2) = |a_{\text{NR}}|^2 + \sum_r |a_r|^2 |A_r(m_+^2, m_-^2)|^2. \quad (5)$$

We find that the model describes the D^0 sideband data well if we include $K^*(892)^-$, $K^*(892)^+$, $K_0^*(1430)^-$, $\rho(770)$, $\rho(1450)$ and σ resonances in the model. We also check that the Dalitz distribution is independent of the tagging category, the flavor tag, and Δt .

Based on a study using the generic Monte Carlo samples, the background with a real D^0 comes mostly from $c\bar{c}$ continuum events. We therefore model the Δt distribution with a prompt component convolved with a core Gaussian plus outlier resolution function. The parameters are determined from the generic Monte Carlo sample.

The Dalitz model for this background is either $A_D(m_+^2, m_-^2)$ or $A_{\bar{D}}(m_+^2, m_-^2)$ based on the flavor of the tagging side B_{tag} . If B_{tag} is tagged as B^0 (\bar{B}^0), the D in the reconstructed candidate is more likely to be a D^0 (\bar{D}^0). Since they are not $B\bar{B}$ events, the mistag rates are not the same as those for the signal. However, we don't have reliable mistag values for continuum events. We therefore use the mistag rates for signal in the nominal fit and vary them to estimate the systematic uncertainty.

The peaking background being mostly from charged B decays, the Δt model is an exponential decay with the lifetime fixed at the B^+ lifetime. The Dalitz model is identical to that for combinatorial background with real D^0 , except that the mistag rates can be different. Again we fix the mistag rates to those for the signal, and vary them for systematic uncertainty.

In the nominal fit, we allow $\cos 2\beta$, $\sin 2\beta$ and $|\lambda|$ to float and fit to all data samples and tagging categories simultaneously. The B^0 lifetime and mixing frequency are fixed at the PDG values. The fit results are shown in Table 2, where the result for which the $\sin 2\beta$ is fixed at the world average and $|\lambda|$ at one is also included. We also allow the m_{ES} shape and background fractions to float in the fit. We find no significant difference in either the central values or the statistical uncertainties. The projections on the Dalitz plot variables are shown in Figure 5 and are compared with the distributions described by the model. Figure 6 shows the time-dependent CP asymmetry for events in $D^0 \rightarrow K_s^0 \rho(770)$ region ($|m(\pi^+ \pi^-) - 0.77| < 0.25 \text{ GeV}/c^2$), where the CP asymmetry is expected to be enhanced. The apparent asymmetry in Figure 6 is small compared to $\sin 2\beta$ due to the dilution factors from mistagging, background and contributions from non-resonance and resonances other than ρ .

Table 2: Results of the fits to data. Errors are statistical only.

Final state	$\cos 2\beta$	$\sin 2\beta$	$ \lambda $
$D^0 \pi^0$	$1.1^{+0.8}_{-0.9}$	1.0 ± 0.5	$1.13^{+0.17}_{-0.14}$
$D^0 \eta^{(\prime)}$	0.4 ± 1.1	$-0.1^{+0.9}_{-1.0}$	$0.96^{+0.19}_{-0.16}$
$D^0 \omega$	$-0.4^{+1.3}_{-1.4}$	0.7 ± 1.0	$0.61^{+0.17}_{-0.15}$
$D^{*0} \pi^0 / \eta$	0.3 ± 1.4	$-0.8^{+1.0}_{-0.9}$	$1.05^{+0.33}_{-0.25}$
All	0.54 ± 0.54	0.45 ± 0.35	0.98 ± 0.09
All	0.55 ± 0.52	0.685 (fixed)	1 (fixed)

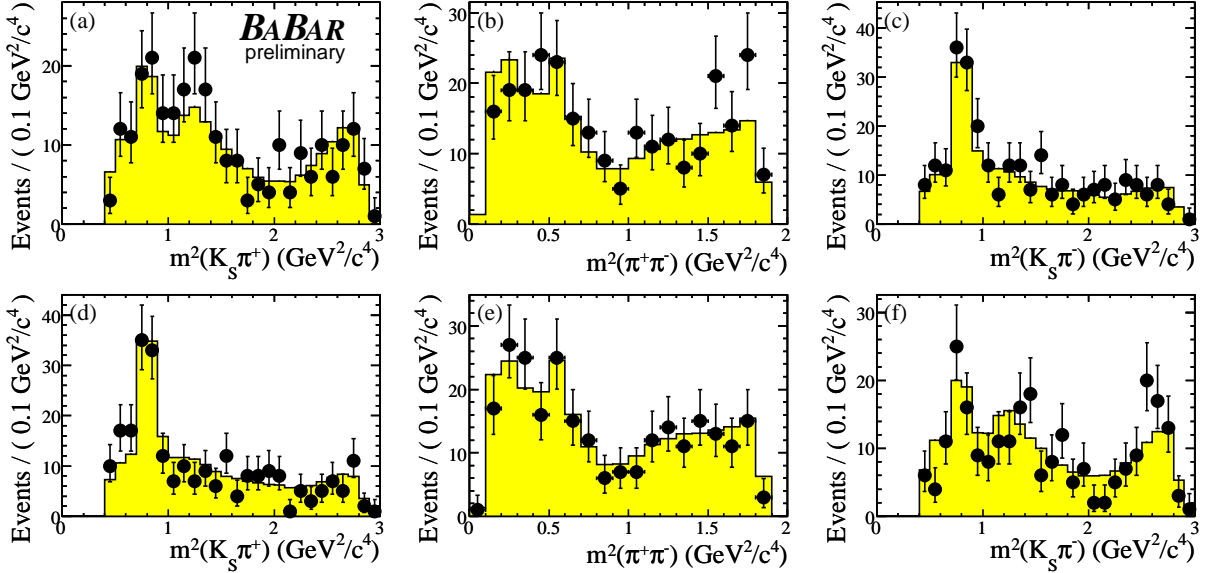


Figure 5: Projection on (a,d) $m_{K_s^0 \pi^+}^2$, (b,e) $m_{\pi^+ \pi^-}^2$, and (c,f) $m_{K_s^0 \pi^-}^2$ for (a,b,c) B^0 -tagged and (d,e,f) \bar{B}^0 -tagged events separately, in the signal region ($m_{\text{ES}} > 5.27 \text{ GeV}/c^2$, $|m_{D^0} - m_{D^0}^{\text{PDG}}| < 20 \text{ MeV}/c^2$). Points with error bars are data; histograms are from the PDF.

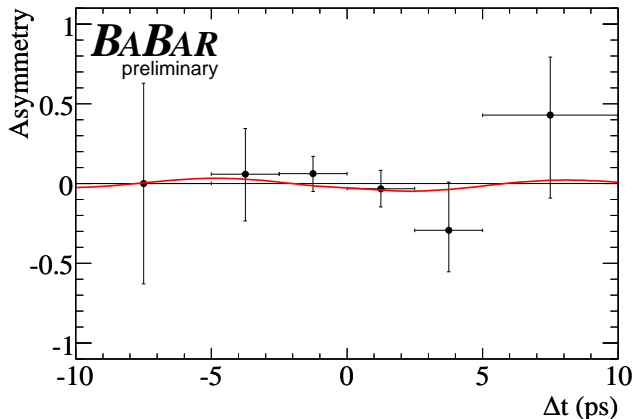


Figure 6: Asymmetry distribution for the events in $D^0 \rightarrow K_s^0 \rho(770)$ region. The curve is the result of the PDF.

6 SYSTEMATIC STUDIES

Dependence on the choice of Dalitz plot model in signal is expected to be one of the largest systematic uncertainties. We estimate the systematic uncertainty by comparing the nominal Dalitz model and an alternative model where the two scalar resonances σ and σ' are removed. We generate 300 toy datasets using the parameters from the nominal fit; each toy dataset has 50 times the data size. We fit to each toy dataset using both nominal Dalitz model and the alternative Dalitz model. We find that both $\sin 2\beta$ and $\cos 2\beta$ shift significantly. We take the quadratic sum of the mean and RMS of the distribution of the difference between the two models as the systematic uncertainty due to Dalitz model uncertainty. The detector resolution on the Dalitz plot is neglected. Only $\omega(782)$ has an intrinsic width comparable to the mass resolution. We increase its width from 8.5 MeV to 10 MeV and find no significant change in the results.

As described in Equation(5), the background Dalitz model is described by an ad hoc incoherent mixture of several resonances and a phase-space distribution. Alternatively, we use a background model containing only K^* and a phase-space distribution to describe the D^0 sideband Dalitz distribution. This model describes the data rather poorly. However, the changes to the final results are quite small.

We vary the B^0 lifetime and mixing by their uncertainty quoted in the PDG [20], and other fixed parameters by their statistical uncertainty in the fits to control samples, to estimate the systematic uncertainties. The parameters include the amplitudes and phases of the Dalitz model, m_{ES} , m_{D^0} and background Δt distributions, background fractions, mistag rates and resolution functions. In addition, we vary several resolution function parameters that were fixed in the fit to the control sample: outlier bias from -2 to $+2$ ps, outlier width from 4 to 12 ps, and the second Gaussian scale factor from 2 to 5.

The mistag rates in both peaking and combinatorial background with a real D^0 are the same as the signal mistag rates in the nominal fit. We vary the mistag rate of each tagging category by $\pm 30\%$ for both backgrounds to estimate the systematic uncertainties.

We fit a two-dimensional third-order polynomial to signal Monte Carlo samples to parametrize the reconstruction efficiency variation over the Dalitz plot. We vary the parameters by their one-sigma statistical uncertainty and the variation in the final answer is again negligible. If we simply

assume the efficiency is a constant across the Dalitz plot, the changes to the results are still quite small and we treat these differences as systematic uncertainties. The systematic uncertainties are summarized in Table 3.

Table 3: Summary of systematic uncertainties.

Item	$\cos 2\beta$	$\sin 2\beta$	$ \lambda $
Signal Dalitz model	0.184	0.073	0.002
Signal Dalitz parameters	0.068	0.026	0.006
Background Dalitz parameters	0.002	0.001	0.002
Background Dalitz model	0.004	0.006	0.008
Δm	0.003	0.002	0.000
τ_{B^0}	0.003	0.001	0.000
τ_{B^+}	0.003	0.000	0.000
Mistag, resolution, etc.	0.043	0.043	0.002
Peaking background fraction	0.020	0.018	0.005
Mistag in combinatorial background with D^0	0.002	0.001	0.001
Mistag in peaking background	0.002	0.001	0.001
Dalitz plot efficiency	0.002	0.001	0.000
Total (non-Dalitz-model)	0.083	0.054	0.012
Total	0.202	0.091	0.012

7 RESULTS

We have measured the CKM phase $\cos 2\beta$ and $\sin 2\beta$ using a time-dependent Dalitz plot analysis of $D^0 \rightarrow K_s^0 \pi^+ \pi^-$ decays in $B^0 \rightarrow D^0 h^0$ decays. We obtain

$$\cos 2\beta = 0.54 \pm 0.54 \pm 0.08 \pm 0.18 \quad (6)$$

$$\sin 2\beta = 0.45 \pm 0.35 \pm 0.05 \pm 0.07 \quad (7)$$

$$|\lambda| = 0.975_{-0.085}^{+0.093} \pm 0.012 \pm 0.002, \quad (8)$$

where the first error is statistical, the second is experimental systematic uncertainty, and the third is the signal Dalitz plot model uncertainty. The statistical correlation between $\cos 2\beta$ and $\sin 2\beta$ is 7%, and less than 5% between $|\lambda|$ and $\cos 2\beta$ or $\sin 2\beta$. The result is consistent with $\sin 2\beta_0 = 0.685 \pm 0.032$ and $\cos 2\beta_0 = \pm \sqrt{1 - \sin^2 2\beta_0} = \pm 0.729$ obtained from high precision measurement using B^0 to charmonium K^0 decays, and consistent with no CP violation in B decay ($|\lambda| = 1$). If $\sin 2\beta$ is fixed at 0.685 and $|\lambda|$ at one in our analysis, we obtain

$$\cos 2\beta = 0.55 \pm 0.52 \pm 0.08 \pm 0.18. \quad (9)$$

This result allows one to distinguish the two possible solutions of angle $2\beta_0$. We generate 1500 parametrized simulation samples of the same size as the data sample, where we use $\sin 2\beta = \sin 2\beta_0$, $\cos 2\beta = |\cos 2\beta_0|$ and $|\lambda| = 1$. We then fit to each sample with $\cos 2\beta$ as the only free parameter, and use a two-Gaussian function $h_+(x)$ to fit to the distribution of the 1500 results. We repeat the

same exercise using $\cos 2\beta = -|\cos 2\beta_0|$ to generate simulation samples and obtain another two-Gaussian distribution $h_-(x)$. The distributions are shown in Figure 7. We define the confidence level (CL) at which the $\cos 2\beta = -|\cos 2\beta_0|$ solution is excluded when we observe $\cos 2\beta = x$ as $h_+(x)/[h_+(x) + h_-(x)]$. We calculate the CL for $\cos 2\beta = 0.55, 0.35$ and 0.75 to account for the systematic uncertainty and use the smallest value, 87%, as the final result.

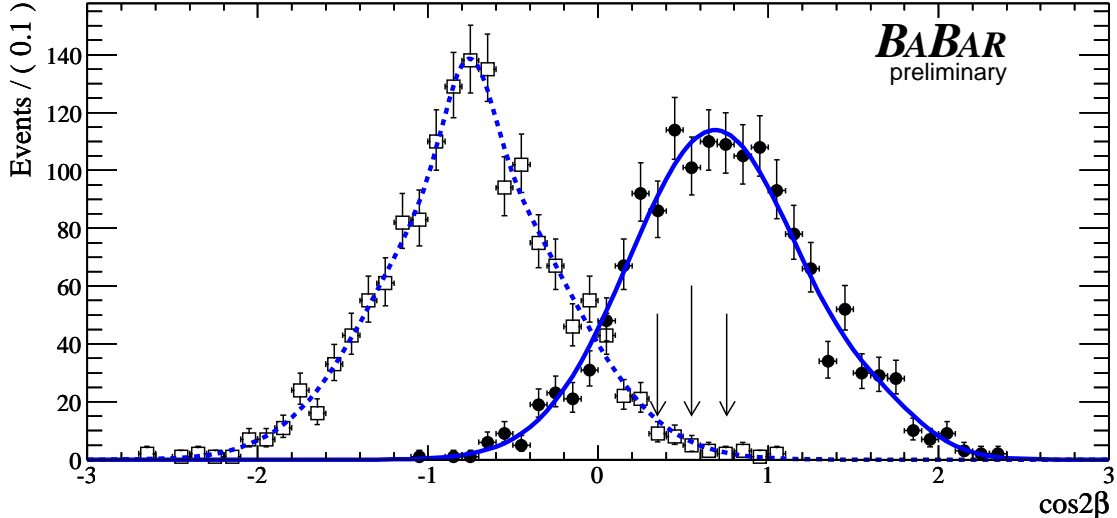


Figure 7: Distribution of $\cos 2\beta$ obtained from two sets of 1500 simulated experiments of the same size as the data sample, as described in the text. Distribution in solid dots (open squares) is for samples generated with $\cos 2\beta = |\cos 2\beta_0|$ ($-|\cos 2\beta_0|$). Solid (dashed) curve is the corresponding two-Gaussian function $h_+(x)$ ($h_-(x)$). Three vertical arrows indicate the central value of $\cos 2\beta$ and plus/minus systematic uncertainty.

8 CONCLUSIONS

We have studied the time-dependent Dalitz distribution in $B^0 \rightarrow D^{(*)0}h^0$ decays and determined the CP asymmetry parameters $\sin 2\beta$, $\cos 2\beta$ and $|\lambda|$. The results are consistent with the Standard Model expectations. Assuming $\sin 2\beta$ is equal to $\sin 2\beta_0$ found in B^0 to charmonium K^0 analyses and no CP violation in B decays, we determined that the solution $\cos 2\beta = -\sqrt{1 - \sin^2 2\beta_0}$ is excluded at an 87% confidence level.

9 ACKNOWLEDGMENTS

We are grateful for the extraordinary contributions of our PEP-II colleagues in achieving the excellent luminosity and machine conditions that have made this work possible. The success of this project also relies critically on the expertise and dedication of the computing organizations that support *BABAR*. The collaborating institutions wish to thank SLAC for its support and the kind hospitality extended to them. This work is supported by the US Department of Energy and National Science Foundation, the Natural Sciences and Engineering Research Council (Canada), Institute of High Energy Physics (China), the Commissariat à l’Energie Atomique and Institut

National de Physique Nucléaire et de Physique des Particules (France), the Bundesministerium für Bildung und Forschung and Deutsche Forschungsgemeinschaft (Germany), the Istituto Nazionale di Fisica Nucleare (Italy), the Foundation for Fundamental Research on Matter (The Netherlands), the Research Council of Norway, the Ministry of Science and Technology of the Russian Federation, and the Particle Physics and Astronomy Research Council (United Kingdom). Individuals have received support from the Marie-Curie IEF program (European Union) and the A. P. Sloan Foundation.

References

- [1] N. Cabibbo, Phys. Rev. Lett, **10**, 531 (1963); M. Kobayashi and T. Maskawa, Prog. Theor. Phys. **49**, 652 (1973).
- [2] B. Aubert *et al.*, [BABAR Collaboration], Phys. Rev. Lett. **94**, 161803 (2005); K. Abe *et al.*, [Belle Collaboration], hep-ex/0507037 (2005).
- [3] E. Barberio *et al.*, [HFAG], hep-ex/0603003 and online update at <http://www.slac.stanford.edu/xorg/hfag>.
- [4] B. Aubert *et al.*, [BABAR Collaboration], Phys. Rev. D **71**, 032005 (2005); R. Itoh, Y. Onuki *et al.*, [Belle Collaboration], Phys. Rev. Lett. **95**, 091601 (2005).
- [5] A. Bondar, T. Gershon and P. Krokovny, Phys. Lett. B **624**, 1 (2005).
- [6] P. Krokovny *et al.*, [Belle Collaboration], hep-ex/0605023 (2006).
- [7] Y. Grossman and M. P. Worah, Phys. Lett. B **395**, 241 (1997); R. Fleischer, Phys. Lett. B **562**, 234 (2003).
- [8] B. Aubert *et al.*, [BABAR Collaboration], Phys. Rev. D **70**, 012007 (2004).
- [9] A. Bondar and T. Gershon, Phys. Rev. D **70**, 091503 (2004).
- [10] S. Agostinelli *et al.*, [GEANT4], Nucl. Instrum. Methods A **506**, 250 (2003), and IEEE Trans. Nucl. Sci. **1**, 270 (2006).
- [11] B. Aubert *et al.*, [BABAR Collaboration], Nucl. Instrum. Methods A **479**, 1 (2002).
- [12] Particle Data Group, S. Eidelman *et al.*, Phys. Rev. B **592**, 1 (2004).
- [13] G.C. Fox and S. Wolfram, Phys. Rev. Lett.**41**, 1581 (1978).
- [14] H. Albrecht *et al.*, [ARGUS Collaboration], Z. Phys. C **48**, 543 (1990).
- [15] T. Skwarnicki [Crystal Ball Collaboration], *A Study of the Radiative Cascade Transitions Between the Υ' and Υ Resonances* DESY F31-86-02, Ph.D thesis.
- [16] S. Kopp *et al.*, [CLEO Collaboration], Phys. Rev. D **63**, 092001 (2001); H. Muramatsu *et al.*, [CLEO Collaboration], Phys. Rev. Lett. **89**, 251802 (2002); Erratum-ibid: **90**, 059901 (2003).
- [17] B. Aubert *et al.*, [BABAR Collaboration], Phys. Rev. Lett. **95**, 121802 (2005).
- [18] G. J. Gounaris and J. J. Sakurai, Phys. Rev. Lett. **21**, 244 (1968).

- [19] See, for example, B. Aubert *et al.*, [*BABAR* Collaboration], Phys. Rev. Lett. **94**, 161803 (2005), and the references therein.
- [20] Y.-M. Yao *et al.*, [Particle Data Group], J. Phys. G33, 1 (2006).